Performance of Compact Antenna Arrays with Receive Selection

Aamir Habib, Christian Mehlführer and Markus Rupp
Vienna University of Technology, Institute of Telecommunications
Gusshausstraße 25/389, A-1040 Vienna
email: {ahabib,chmehl,mrupp}@nt.tuwien.ac.at

***Abstract*—The objective of this paper is to evaluate the performance of dual-polarized Multiple-Input Multiple-Output (MIMO) systems, compact in antenna array size and with reduced radio frequency complexity. We compare co-located antenna array structures with their spatial counterpart while deploying receive antenna selection. To this purpose, the performance in terms of MIMO maximum mutual information is presented. A simple norm based on instantaneous channels selects the best antennas. We derive explicit numerical expressions for the effective channel gains. These expressions are precise for small values of N_S and N_R, and approximately valid for higher values of N_S and N_R, N_S and N_R being the number of selected and total receive antennas, respectively. Further a comparison in terms of power imbalance between antenna elements is presented. We conclude that angularly separated compact antenna arrays with a few simple monopoles, if used with antenna selection can provide a better performance compared to a conventional Uniform Linear Array (ULA). We also show that co-located structures are robust to power imbalance and orientation variations compared to a ULA.**

Keywords-Angular diversity, angular correlation, antenna selection, XPD, array orientation, array rotation.

I. Introduction

Achieving high spectral efficiency in Multiple-Input Multiple-Output (MIMO) systems implies the use of multiple antenna elements. However, from the implementation aspects in small hand-held devices, increasing the number of radiating elements may cause design problems. Not only the number of elements but also the spacing between them, can make the compact design very challenging. For a given antenna aperture constraint, increasing the number of antenna elements decreases the amount of spacing thus increasing the correlation. As a rule of thumb the inter-element spacing should be not less than half a wavelength to successfully de-correlate the incoming waves. This, not only imposes challenges for the size of mobile devices but also constraints on Radio Frequency (RF) domain, which in effect causes the number of RF chains to increase as well. To overcome the space limitations in MIMO, there are other ways of providing diversity, such as polarization [1], [2], angle and pattern diversity [3]. Signals from a pair of antennas with orthogonal polarization are combined together to provide polarization diversity. Extensions to three orthogonally polarized antenna elements further augment the degrees of freedom for incoming signals and hence the diversity [4]. Co-located antennas with different radiation patterns can be combined together to provide pattern diversity. Pattern diversity makes use of directional antennas which are physically separated by a very short distance. Similarly co-located radiating elements with different angular spacing can be used to realize angular diversity. One of the main drawbacks of MIMO systems with arrays of parallel dipoles is their sensitivity to a polarization mismatch [5], due to random orientations of the device. To reduce this effect, the benefits of polarization and/or pattern diversity can be exploited [3]. Compact antenna arrays are used to overcome space limitations in small devices, nevertheless conventional MIMO systems require one down-conversion/up-conversion RF chain for each antenna element. While the antenna elements themselves do not increase transceiver costs significantly, the RF chains are a very significant cost factor. Antenna subset selection techniques help in cost reduction for MIMO deployment, while maintaining full MIMO diversity benefits. In [6], [7] selection algorithms for maximizing the channel mutual information are presented together with performance measures. It was proved that the diversity order achievable by antenna selection is the same as that of a full complexity system. In [8], receive antenna subset selection schemes are applied in a MIMO-OFDM transmission system. Simulation results in terms of average throughput and Bit Error Ratio (BER) on an adaptive modulation and coding link have been shown. Various channel models have been used in literature for evaluating multiple antenna systems but for the sake of intuition and to include the effects of antenna geometry, we use the double-directional analytical channel model as investigated in [9]. The advantage of using such model is that it incorporates the following:

- Random mobile terminal rotation effects
- Antenna polarization
- Spatial, pattern and polarization diversity of array.

Other than the above characteristics; the representation is intuitive as shown to be the product of antenna and channel effects. However, in this work we modify the model from its original to include correlation properties between the antenna elements. The values of correlation have been taken from [10]. In this work, models for accurate estimation of correlation for hybrid spatial-angular MIMO systems are given. The model presented in [10] is valid for Rayleigh fading channels and isotropic scatterings. We choose a simple model from that work to obtain the correlation values and include them into our channel model for further analysis. The utilization of

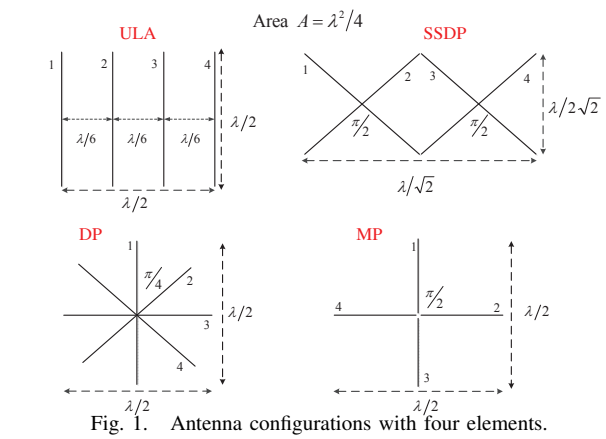

Fig. 1. Antenna configurations with four elements.

multiple polarizations of the electromagnetic wave to extract diversity is well known and understood for a long time. The capacity of the dual polarized MIMO channel is evaluated and compared to the capacity of a single polarized array. In [11], the potential advantages of employing dual-polarized arrays in multi-antenna wireless systems for various channels is studied. In this work we compare four different antenna array configurations at the receive side in terms of capacity of the system, while at the transmit side we use only a single vertically oriented antenna element. The antenna configurations are depicted in Fig. 1. The size of the array aperture is limited to an area of $\frac{\lambda^2}{4}$ for all arrangements, for a fair comparison. Selection of antenna subsets is performed on the basis of the maximum Frobenius norm of rows of channel matrices. For the sake of simplicity we ignore the effects of mutual coupling [12] between the ports of antenna elements.

II. Channel Model

A channel model for N_R receive antennas and a single transmit antenna is given by

$$\tilde{\mathbf{H}} = (\mathbf{P}_{N_R\times 2}\mathbf{G}_{2\times 2}\mathbf{X}_{2\times 1}) \odot \left(\mathbf{R}^{1/2}_{N_R\times N_R}\mathbf{H}_{N_R\times 1}\right), \qquad (1)$$

where

$$\mathbf{P}_{N_R\times 2} = \begin{bmatrix} \cos(\theta_p+\varphi_1) & \sin(\theta_p+\varphi_1) \\ \cos(\theta_p+\varphi_2) & \sin(\theta_p+\varphi_2) \\ \vdots & \vdots \\ \cos(\theta_p+\varphi_{N_R}) & \sin(\theta_p+\varphi_{N_R}) \end{bmatrix},$$

represents the orientation/rotation of the array and the dual polarized nature of each receive antenna element. The $\odot$ operator defines a scalar multiplication [1]. Here, θ_p is the orientation or rotation of the array in space and φ_n is the orientation of individual antenna elements respect to each other and defined in the next section.

$$\mathbf{G}_{2\times 2} = \begin{bmatrix} G_C(\phi) & G_X(\phi) \\ -G_X(\phi) & G_C(\phi) \end{bmatrix},$$

is the gain matrix at azimuth angle ϕ, $G_C(\phi)$ is the co-polar gain pattern and $G_X(\phi)$ is the cross polar component. This matrix depicts the pattern diversity effect.

$$\mathbf{X}_{2\times 1} = \begin{bmatrix} \sqrt{1-\alpha} & \sqrt{\alpha} \end{bmatrix}^{\mathrm{T}},$$

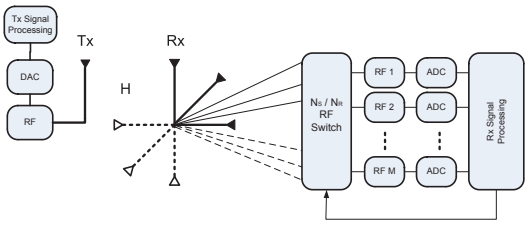

Fig. 2. MIMO system (1 Tx and N_R Rx) with receive antenna selection.

represents the XPD matrix defined in [1], [5], [11] where $0 \leq \alpha \leq 1$ is the amount of power transfered from one antenna element to another. The antenna XPD is specified by $\mathrm{XPD} = \frac{1-\alpha}{\alpha}$. Therefore, when

$$\lim_{\alpha\to 0} \mathrm{XPD} = \infty; \qquad \lim_{\alpha\to 1} \mathrm{XPD} = 0.$$

We assume here an equal antenna XPD loss between each pair of antenna elements. However, a variable XPD loss could also be an interesting work for the future. Here, $\mathbf{H}_{N_R\times 1}$ is the matrix containing i.i.d complex Gaussian fading coefficients and $\mathbf{R}_{N_R\times N_R}$ is the normalized correlation matrix. This matrix is calculated according to the results taken from [10]. The matrix representing the pattern diversity is ignored here for simplification as we consider an omni-directional azimuth gain pattern for both orthogonal components. Therefore here, we only consider the effects of polarization diversity. Hence the model given in Eq. (1) can be simplified to

$$\tilde{\mathbf{H}} = (\mathbf{P}_{N_R\times 2}\mathbf{X}_{2\times 1}) \odot \left(\mathbf{R}^{1/2}_{N_R\times N_R}\mathbf{H}_{N_R\times 1}\right). \qquad (2)$$

The basic transmission system with receive antenna selection is given in Fig. 2. The performance of this MIMO system is calculated on the basis of maximum mutual information. The mutual information is stated below as

$$C = \log_2\det\left(\mathbf{I} + \frac{\rho}{\mathrm{N_T}}\tilde{\mathbf{H}}\tilde{\mathbf{H}}^{\mathrm{H}}\right), \qquad (3)$$

where N_T is the number of transmit antennas and ρ is the mean signal to noise ratio. The performance with receive antenna selection is calculated by selecting those rows of channel matrix $\tilde{\mathbf{H}}$ which have the maximum Frobenius norm and then calculating the maximum mutual information. Thus previous equation with receive antenna selection becomes

$$C_\Lambda = \log_2\det\left(\mathbf{I}_\Lambda + \frac{\rho}{\mathrm{N_T}}\tilde{\mathbf{H}}_\Lambda\tilde{\mathbf{H}}^{\mathrm{H}}_\Lambda\right), \qquad (4)$$

where Λ denotes the receive antenna subset.

III. Correlation of Antenna Arrays

The spatial correlation between two consecutive identical antennas can be found in [10], given as

$$\varsigma = \sin(z_s)/z_s, \qquad (5)$$

and its power is presented in Fig. 3, where $z_s = 2\pi d_s/\lambda$ and d_s is the inter-element distance. The correlation function between antenna elements separated by an angular displacement is established by an equivalence between angular and spatial

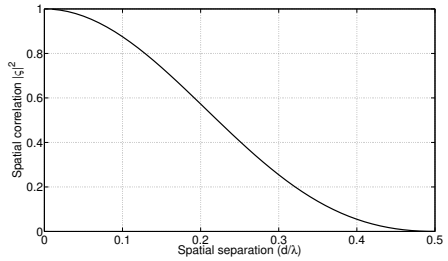

Fig. 3. Spatial correlation function.

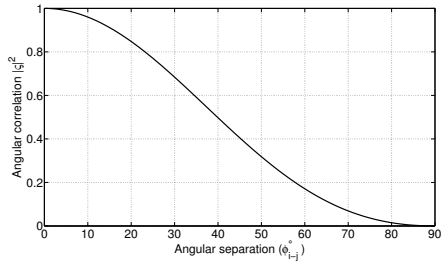

Fig. 4. Angular correlation function.

separation. This is called true polarization diversity [13] and shown below as

$$\varsigma = \sin(z_a)/z_a, \tag{6}$$

where $z_a = 2\pi d_a$. For a small number of receiving antennas and under Rayleigh fading scenarios the angular separation d_a can be made equivalent to a spatial separation by

$$d_a = \varphi_{i-j}/180^\circ, \tag{7}$$

where $\varphi_{i-j} = \varphi_i - \varphi_j$ is the angular difference between two dipoles, and φ_i and φ_j are the orientation angles of dipoles i and j with respect to vertical axis. The power of angular correlation function is shown in Fig. 4.

IV. Antenna Array Configurations

The model presented in the previous section was applied to the four configurations as shown in Fig. 1. Each configuration contains four antenna elements arranged in a different way. The total area or aspect ratio was kept constant so as to have a fair comparison in terms of performance. The first array is the most common setting with spatially separated dipole arrays spaced equally apart with inter-element distance of $\lambda/6$. The second configuration contains a pair of cross dipoles. The centers of the dipoles are separated by a distance of $\lambda/(2\sqrt{2})$. In the third configuration we have an arrangement of dipoles whose centers or feed points are co-located with no inter-element distance. All the dipoles are separated with an angular displacement as defined in the previous section. The last configuration contains an array of monopoles whose edges are co-located. We have assumed here that the ground planes for each monopole are somehow separated from each other. The correlations are defined again according to the angular displacement rather than spatial. Dipoles and monopoles mentioned in the last three configurations produce various patterns due to slant angles hence introducing both pattern and polarization diversity, but here for the sake of simplicity we assume only polarization diversity. Effects of pattern diversity would be discussed in future work. In all of our work we consider a single vertical antenna at the transmit side. Extension to multiple transmit antennas with various transmission strategies can also be exploited. As an explanation of the construction of the correlation matrix $\mathbf{R}_{N_R \times N_R}$ we take the example of a spatially separated cross dipole array. The angular separation between each pair of dipoles is $\varphi = 90^\circ$. $\varphi_{1-2} = \varphi_1 - \varphi_2 = \varphi_{3-4} = \varphi_3 - \varphi_4 = 90^\circ$. And $d_1 = \varphi_{1-2}/180^\circ = d_2 = \varphi_{3-4}/180^\circ = 1/2$. The angular correlation coefficients $\varsigma = \sin(z_a)/z_a = 0$. As the pairs are separated by a spatial distance of $\lambda/(2\sqrt{2})$, the spatial correlation coefficient is given by $\varsigma = \sin(\pi/\sqrt{2})/(\pi/\sqrt{2}) = 0.3582$. The total normalized correlation matrix is given by the Kronecker product of two correlation matrices $\mathbf{R}_{\mathrm{SSDP}} = \mathbf{R}_{\mathrm{sp}}^{1/2} \otimes \mathbf{R}_{\mathrm{cp}}^{1/2} / \left\| \mathbf{R}_{\mathrm{sp}}^{1/2} \otimes \mathbf{R}_{\mathrm{cp}}^{1/2} \right\|$ with

$$\mathbf{R}_{\mathrm{sp}} = \begin{bmatrix} 1 & 0.3582 \\ 0.3582 & 1 \end{bmatrix}, \tag{8}$$

and

$$\mathbf{R}_{\mathrm{cp}} = \begin{bmatrix} 1 & 0 \\ 0 & 1 \end{bmatrix}, \tag{9}$$

where $\mathbf{R}_{\mathrm{cp}}$ and $\mathbf{R}_{\mathrm{sp}}$ are the correlation matrices for cross dipoles and spatially separated dipoles, respectively. The complete matrix is given below.

$$\mathbf{R}_{\mathrm{SSDP}} = \begin{bmatrix} 0.844 & 0 & 0.156 & 0 \\ 0 & 0.844 & 0 & 0.156 \\ 0.156 & 0 & 0.844 & 0 \\ 0 & 0.156 & 0 & 0.844 \end{bmatrix}, \tag{10}$$

V. Theoretical Analysis

In order to find algebraic expressions we analyze effective channel gains on the example of monopoles. The same procedure can be adopted for other configurations. The theoretical work presented here is along the sames lines as in [14]. In [14] only one structure of an antenna array was analyzed. The model for a generic $1 \times N_R$ Single-Input Multiple-Output (SIMO) system with Maximum Ratio Combining (MRC) is explained in the following. Subsequently a model for Receive Antenna Selection (RAS) with MRC will be shown. The channel matrix is written as

$$\mathbf{h} = [h_1, h_2, \cdots, h_{N_R}]^{\mathrm{T}},$$

and the received signal vector by

$$\mathbf{y} = \mathbf{h} \cdot x + \mathbf{v}, \tag{11}$$

where $x \in \mathcal{C}$ and $\mathbf{v} \in \mathcal{C}^N$ with $\mathbf{v}$ being a noise vector with i.i.d and circularly symmetric complex-valued Gaussian entries with variance 1/2 σ_v^2 for each real dimension. The detected symbol at the MRC output is shown as

$$\hat{x} = \mathbf{h}^{\mathrm{H}} \cdot \mathbf{h} \cdot x + \mathbf{h}^{\mathrm{H}} \cdot \mathbf{v}, \tag{12}$$

where $(\cdot)^{\mathrm{H}}$ denotes the Hermitian. The received signal for receive antenna selection is then given by

$$\mathbf{y}^{(\mathcal{S}_{\mathcal{N}_\mathcal{S}})} = \mathbf{h}^{(\mathcal{S}_{\mathcal{N}_\mathcal{S}})} \cdot x + \mathbf{v}^{(\mathcal{S}_{\mathcal{N}_\mathcal{S}})}, \tag{13}$$

where the MRC only combines the received signals from the selected antennas identified by the set of indices of an ordered set $\mathcal{S}_{\mathcal{N}_S} = \{n_1, n_2, \cdots, n_{N_S}\}$ where $n_i \in [1, 2, \cdots, N_R]$. The detected symbol after receive antenna selection is then

$$\hat{x}^{(\mathcal{S}_{\mathcal{N}_S})} = \mathbf{h}^{(\mathcal{S}_{\mathcal{N}_S})\mathrm{H}} \cdot \mathbf{h}^{(\mathcal{S}_{\mathcal{N}_S})} \cdot x + \mathbf{h}^{(\mathcal{S}_{\mathcal{N}_S})\mathrm{H}} \cdot \mathbf{v}, \tag{14}$$

The gain of full complexity receiver is given by

$$G_{N_R/N_R} = E\left[\mathbf{h}^{\mathrm{H}} \cdot \mathbf{h}\right], \tag{15}$$

while the gain of receiver with antenna selection is given by

$$G_{N_S/N_R} = E\left[\mathbf{h}^{(\mathcal{S}_{\mathcal{N}_S})\mathrm{H}} \cdot \mathbf{h}^{(\mathcal{S}_{\mathcal{N}_S})}\right]. \tag{16}$$

The channel matrix for 1×4 SIMO, following the model defined in Eq. (2)

$$\mathbf{h}_{4\times 1} = \begin{bmatrix} h_1\left(\sqrt{1-\alpha}\cos(\phi_1) + \sqrt{\alpha}\sin(\phi_1)\right) \\ h_2\left(\sqrt{1-\alpha}\cos(\phi_2) + \sqrt{\alpha}\sin(\phi_2)\right) \\ h_3\left(\sqrt{1-\alpha}\cos(\phi_3) + \sqrt{\alpha}\sin(\phi_3)\right) \\ h_4\left(\sqrt{1-\alpha}\cos(\phi_4) + \sqrt{\alpha}\sin(\phi_4)\right) \end{bmatrix}, \tag{17}$$

where $\phi_n = \theta + \varphi_{i-j}$ and φ_{i-j} is defined in Eq. (7) earlier. The channel coefficients h_1, h_2, h_3, h_4 contain the effects of correlation, calculated from Eq. (5) and Eq. (6) for various antenna configurations. As we have realized an MRC receiver, we sum the squares of the channel coefficients for each row of the channel matrix in Eq. (17) and take the average over all realizations. The effective channel gain is then shown by Eq. (20). We analyze $1/4$ and $N_S/4$ RAS with polarization next. We start by selecting $N_S = 1$ out of 4 from the channel matrix given by Eq. (17), with the largest norm, $\bar{n} \in [1, 2, 3, 4]$ being the index of the selected antenna element. The corresponding channel coefficient $h_{1/4}$ becomes a scalar.

$$h_{1/4} = \left[h_{\overline{n}}\left(\sqrt{1-\alpha}\cos\left(\phi_{\overline{n}}\right) + \sqrt{\alpha}\sin\left(\phi_{\overline{n}}\right)\right)\right], \tag{18}$$

the effective channel gain is expressed in Eq. (21) and an approximate value in Eq. (22). A similar matrix $\mathbf{h}_{N_S/4} = [h_1, h_2, h_3, h_4]^T$ can be constructed, containing only the channel coefficients of the N_S selected antenna elements, indices of which would be from an ordered set given by $\mathcal{S}_{\mathcal{N}_S} = \{n; \|h_n\|_F > \|h_{N_S+1}\|_F\} = [n_1, n_2, \cdots, n_{N_S}]$. The new channel matrix with $N_S/4$ selection is then given by

$$\mathbf{h}_{N_S/4} = \begin{bmatrix} h_{n_1}\left(\sqrt{1-\alpha}\cos(\phi_1) + \sqrt{\alpha}\sin(\phi_1)\right) \\ h_{n_2}\left(\sqrt{1-\alpha}\cos(\phi_2) + \sqrt{\alpha}\sin(\phi_2)\right) \\ h_{n_3}\left(\sqrt{1-\alpha}\cos(\phi_3) + \sqrt{\alpha}\sin(\phi_3)\right) \\ h_{n_4}\left(\sqrt{1-\alpha}\cos(\phi_3) + \sqrt{\alpha}\sin(\phi_4)\right) \end{bmatrix}, \tag{19}$$

For a monopole configuration, the correlation matrix $\mathbf{R} = \mathbf{I}$, because all $\varsigma's = 0$ from Eq. (6). The channel gains are dependent, both on rotation and XPD. Here, for the sake of simplicity we do average only over rotation while keeping $\alpha = 0$. The same analysis can be performed for other values of α and then averaged. Now for $1/4$ RAS we do the following. As $E\left\|h_1^2\right\| = E\left\|h_2^2\right\| = E\left\|h_3^2\right\| = E\left\|h_4^2\right\| = 1$ for Rayleigh fading channels, we deduce the following inequality from an approximation of Eq. (22). We solve it for $\alpha = 0$ and get $\cos^2\theta_p > \cos^2\left(\theta_p + \frac{\pi}{2}\right) > \cos^2\left(\theta_p + \frac{2\pi}{2}\right) > \cos^2\left(\theta_p + \frac{3\pi}{2}\right)$. This results in the interval $0 < \theta_p < \frac{\pi}{4}$ so

$$G_{1/4,\alpha=0} = \frac{4}{\pi}\int_0^{\frac{\pi}{4}} \left(\cos^2\theta_p\right) d\theta_p = 0.8183.$$

Similarly solving for $2/4$ RAS we have $\cos^2\left(\theta_p + \frac{\pi}{2}\right) > \cos^2\left(\theta_p + \frac{2\pi}{2}\right) > \cos^2\left(\theta_p + \frac{3\pi}{2}\right)$. We get the interval as $\frac{\pi}{4} < \theta_p < \frac{\pi}{2}$. We have

$$G_{2/4,\alpha=0} = \frac{4}{\pi}\int_0^{\frac{\pi}{4}} \left(\cos^2\theta_p\right) d\theta_p + \frac{4}{\pi}\int_{\frac{\pi}{4}}^{\frac{\pi}{2}} \cos^2\left(\theta_p + \frac{\pi}{2}\right) d\theta_p = 1.628.$$

Calculating in the similar fashion we have for $3/4$ RAS shown in Eq. (23). For full complexity SIMO we have the relation depicted in Eq. (24). The theoretical results for the case of monopole configuration are compared with the simulation in Fig. 5. Analysis with the same method for other configurations can be easily performed but not shown here due to space limitations.

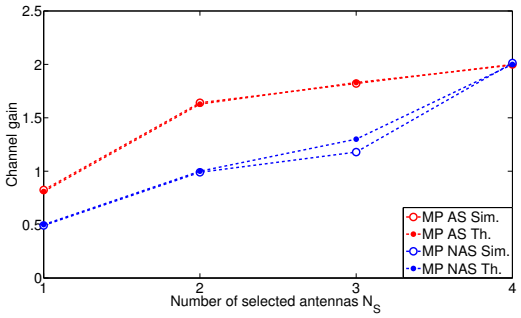

Fig. 5. Comparison of monopole array with $N_S/4$ selection and N_R/N_R full complexity array at 30 dB SNR.

VI. Simulation Results

Simulation results are shown in terms of mutual information, both with and without receive antenna selection. Here, N_S is the number of antennas to be selected and N_R is the total number of antennas available. Also, N_S/N_R denotes the selection of N_S antenna elements out of N_R elements. The results are shown for various performance parameters. The two most important parameters are the XPD and the rotation. In the figures shown next we perform simulations considering these parameters. In Fig. 6 we show the comparison between the configurations of Fig. 1. We show the performance for a full complexity system as well as for receive antenna selection. From the figure we observe that the configuration with monopole structure has the maximum mutual information when used in conjunction with selection. Construction of such array is practically very difficult but due to very less angular correlation, it performs better compared to other structures. For a full complexity system, the SSDP configuration performs better. Although for a ULA the mutual information increases while increasing N_S but the performance degrades for values of $3/3$ and $4/4$ full complexity system. This is due to inter-element distance becoming less than $\lambda/2$. In the Fig. 7 we compare $2/4$ selection for various antenna configurations. NAS in the simulation represents a full complexity system with no antenna selection. From the figure we observe that

$$G_{N_R/N_R}(\theta_p) = \sum_{n=1}^{N_R} E\left[|h_n|^2 \left(\sqrt{1-\alpha}\cos\left(\theta_p + \frac{(n-1)2\pi}{N_R}\right) + \sqrt{\alpha}\sin\left(\theta_p + \frac{(n-1)2\pi}{N_R}\right)\right)^2\right]. \tag{20}$$

$$G_{1/N_R}(\theta_p) = E\left[\max\left\{|h_1|^2\left(\sqrt{1-\alpha}\cos\left(\phi_1\right) + \sqrt{\alpha}\sin\left(\phi_1\right)\right)^2, \cdots, |h_{N_R}|^2\left(\sqrt{1-\alpha}\cos\left(\phi_{N_R}\right) + \sqrt{\alpha}\sin\left(\phi_{N_R}\right)\right)^2\right\}\right]. \tag{21}$$

$$G_{1/N_R}(\theta_p) \approx \max\left\{E\left[|h_1|^2\right]\left(\sqrt{1-\alpha}\cos\left(\phi_1\right) + \sqrt{\alpha}\sin\left(\phi_1\right)\right)^2, \cdots, E\left[|h_{N_R}|^2\right]\left(\sqrt{1-\alpha}\cos\left(\phi_{N_R}\right) + \sqrt{\alpha}\sin\left(\phi_{N_R}\right)\right)^2\right\}. \tag{22}$$

$$G_{3/4,\alpha=0} = \frac{4}{\pi}\int_0^{\frac{\pi}{4}} \left(\cos^2\theta_p\right) d\theta_p + \frac{4}{\pi}\int_{\frac{\pi}{4}}^{\frac{\pi}{2}} \cos^2\left(\theta_p + \frac{\pi}{2}\right) d\theta_p + \frac{4}{\pi}\int_{\frac{\pi}{4}}^{\frac{\pi}{2}} \cos^2\left(\theta_p + \frac{3\pi}{2}\right) d\theta_p = 1.83. \tag{23}$$

$$G_{N_R/N_R} = \frac{2}{\pi}\int_0^{\frac{\pi}{2}} \left[\sum_{n=1}^{N_R} E\left\{|h_n|^2\left(\sqrt{1-\alpha}\cos\left(\theta_p + \frac{(n-1)2\pi}{N_R}\right) + \sqrt{\alpha}\sin\left(\theta_p + \frac{(n-1)2\pi}{N_R}\right)\right)^2\right\}\right] d\theta_p. \tag{24}$$

the mutual information of a ULA is strongly deteriorated by a decrease in the XPD. The performance of both monopole and dipole structure is similar. The mutual information decreases for decreasing XPD but again increases for lower values of XPD. Thus all the structures other than ULA, are robust to power imbalance between dual polarized antenna elements. In Fig. 8 we compare a $2/4$ selection for various antenna configurations by varying the orientation angle of the structures. We observe from the figure that again the ULA is effected by the orientation angle and other structures are almost insenstitve to the change in orientation. From the previous two figures we also observe that mutual information depends both on array orientation as well as XPD. In Figures 9, 10, 11, 12 we show the mutual information with selection for various configurations and its dependence on both XPD and orientation. The variation of mutual information in dipole configuration is very less when compared to the monopole structure, but its behavior is different. The dipole configuration has four minimum and maximum contour lines. The monopoles have three maximum and two minimum contours. The variation along rotation and XPD for SSDP configuration is opposite to monopole configurations with two maximum and three minimum contour lines. The ULA configuration is badly effected by higher values of both rotation and XPD. The performance degrades quickly after the values of $\alpha = 0.6$ and $\psi = 60^o$. From Fig. 6 we see that the arrangement with monopoles shows the best performance with antenna selection. This is because the selection process always selects either Antenna 1 or 3 in case of $1/4$ selection, which are highly un-correlated. Its performance is better in average as compared to dipole configuration because for dipole, always Antenna 1 is selected, which is always vertical oriented. The performance of the SSDP configuration is better than dipoles because on average, either Antennas 1 or 3 is selected which are both inclined by 45° and also spatially separated. The ULA performs the worst as all the antenna are selected on average. The same intuitive reasoning can be applied for the $2/4$ and $3/4$ selection. The performance is different for full complexity systems on the average. As an example if we take a three antenna full complexity system, SSDP reveals the best performance because it is constructed from two orthogonal antennas with an additional spatially separated and 45°inclined antenna. The mutual information for monopoles is slightly

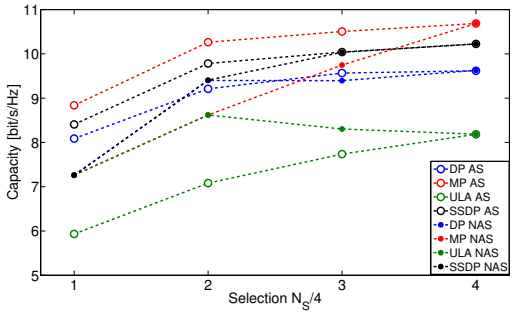

Fig. 6. Comparison of antenna configurations with $N_S/4$ receive antenna selection at 30 dB SNR and averaged over 90° rotation.

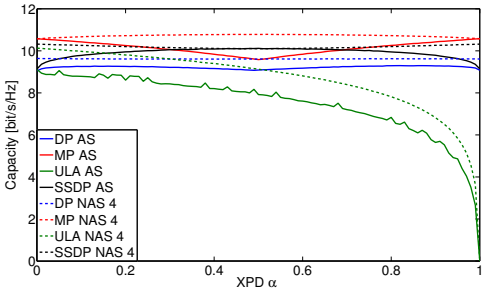

Fig. 7. Comparison of antenna configurations with 2/4 selection with varying XPD at 30 dB SNR and $\Psi = 0$.

better than that of a dipole arrangement because all the three antennas are separated 90° apart compared to 60° separation for a dipole configuration. The ULA performance is degraded due to decreasing spatial distance and hence an increase in correlation.

VII. Conclusions

We compared four different antenna configurations in terms of mutual information with receive antenna selection and full complexity systems. We studied their performance in terms of mutual information of the antenna arrays, with and without receive antenna selection for all the arrangements. An analysis averaged over rotation and XPD was also simulated separately. A combined effect of rotation and XPD was presented. Analytical expressions for channel gains with and without antenna selection were presented. A comparison of simulation results with theoretical results was shown.

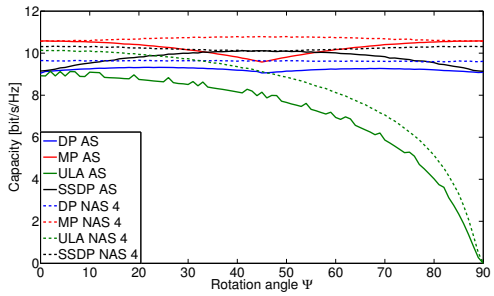

Fig. 8. Comparison of antenna configurations with 2/4 selection with varying rotation at 30 dB SNR and $\alpha = 0$.

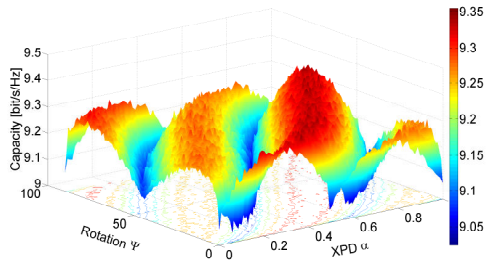

Fig. 9. Dipole antenna configuration with 2/4 selection with varying rotation and XPD at 30 dB SNR.

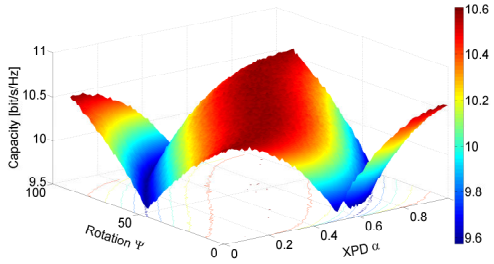

Fig. 10. Monopole antenna configuration with 2/4 selection with varying rotation and XPD at 30 dB SNR.

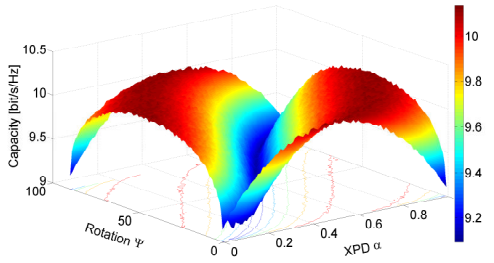

Fig. 11. Spatially separated dipole antenna configuration with 2/4 selection with varying rotation and XPD at 30 dB SNR.

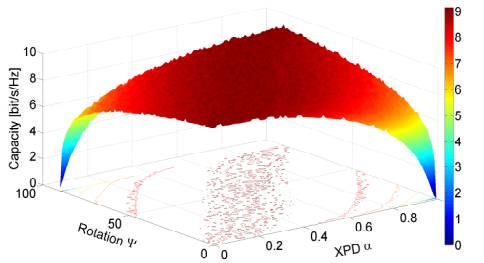

Fig. 12. Uniform linear array antenna configuration with 2/4 selection with varying rotation and XPD at 30 dB SNR.

ACKNOWLEDGMENTS

This work has been funded by the Christian Doppler Laboratory for Wireless Technologies for Sustainable Mobility, KATHREIN-Werke KG, and A1 Telekom Austria AG. The financial support by the Federal Ministry of Economy, Family and Youth and the National Foundation for Research, Technology and Development is gratefully acknowledged. The authors would like to thank Christoph F. Mecklenbräuker for his valuable comments and fruitful discussions. This work has also been funded by the Higher Education Commission, Islamabad, Pakistan.

REFERENCES

[1] M. Coldrey, "Modeling and capacity of polarized MIMO channels," in *Proc. IEEE Vehicular Technology Conf. VTC Spring 2008*, 2008, pp. 440–444.

[2] W. Lee and Y. Yeh, "Polarization diversity system for mobile radio," *IEEE Transactions on Communications*, vol. 20, no. 5, pp. 912–923, 1972.

[3] C. Waldschmidt, C. Kuhnert, S. Schulteis, and W. Wiesbeck, "Compact MIMO-arrays based on polarisation-diversity," in *Proc. IEEE Antennas and Propagation Society Int. Symp*, vol. 2, 2003, pp. 499–502.

[4] T. Svantesson, "On capacity and correlation of multi-antenna systems employing multiple polarizations," in *Proc. IEEE Antennas and Propagation Society Int. Symp*, vol. 3, 2002.

[5] M. Shafi, M. Zhang, A. L. Moustakas, P. J. Smith, A. F. Molisch, F. Tufvesson, and S. H. Simon, "Polarized MIMO channels in 3-D: models, measurements and mutual information," *IEEE Journal on Selected Areas in Communications*, vol. 24, pp. 514–527, 2006.

[6] A. Gorokhov, D. A. Gore, and A. J. Paulraj, "Receive antenna selection for MIMO spatial multiplexing: theory and algorithms," *IEEE Transactions on Signal Processing*, vol. 51, no. 11, pp. 2796–2807, 2003.

[7] D. A. Gore and A. J. Paulraj, "MIMO antenna subset selection with space-time coding," *IEEE Transactions on Signal Processing*, vol. 50, no. 10, pp. 2580–2588, 2002.

[8] A. Habib, C. Mehlführer, and M. Rupp, "Performance comparison of antenna selection algorithms in WiMAX with link adaptation," in *Proc. 4th Int. Conf. Cognitive Radio Oriented Wireless Networks and Communications CROWNCOM '09*, 2009, pp. 1–5.

[9] R. Bhagavatula, C. Oestges, and R. W. Heath, "A new double-directional channel model including antenna patterns, array orientation, and depolarization," *IEEE Transactions on Vehicular Technology*, vol. 59, no. 5, pp. 2219–2231, 2010.

[10] J. F. Valenzuela-Valdes, A. M. Martinez-Gonzalez, and D. A. Sanchez-Hernandez, "Accurate estimation of correlation and capacity for hybrid spatial-angular MIMO systems," *IEEE Transactions on Vehicular Technology*, vol. 58, no. 8, pp. 4036–4045, 2009.

[11] C. Oestges, B. Clerckx, M. Guillaud, and M. Debbah, "Dual-polarized wireless communications: from propagation models to system performance evaluation," *IEEE Transactions on Wireless Communications*, vol. 7, no. 10, pp. 4019–4031, 2008.

[12] H. Li, G. Zhaozhi, M. Junfei, J. Ze, L. ShuRong, and Z. Zheng, "Analysis of mutual coupling effects on channel capacity of MIMO systems," in *Proc. IEEE Int. Conf. Networking, Sensing and Control ICNSC 2008*, 2008, pp. 592–595.

[13] J. F. Valenzuela-Valdes, M. A. Garcia-Fernandez, A. M. Martinez-Gonzalez, and D. Sanchez-Hernandez, "The role of polarization diversity for MIMO systems under Rayleigh-fading environments," *IEEE Antennas and Wireless Propagation Letters*, vol. 5, no. 1, pp. 534–536, 2006.

[14] A. Habib, C. Mehlführer, and M. Rupp, "Receive antenna selection for polarized antennas," in *Proceedings of 18th International Conference on Systems, Signals and Image Processing*, Sarajevo, Bosnia, June 2011.